RAA 2021 Vol. **21** No. **3**, 53(13pp) doi: 10.1088/1674-4527/21/3/53

http://www.raa-journal.org *http://iopscience.iop.org/raa*

Research in Astronomy and Astrophysics

Temporal variation of solar flare index during solar cycles 21 – 24

Soumya Roy[1], Amrita Prasad[2], Subhash Chandra Panja[2] and Sankar Narayan Patra[3]

[1] Department of Applied Electronics and Instrumentation Engineering, Haldia Institute of Technology, Haldia, Midnapore (E) - 721657, West Bengal, India; *er.sroy9@gmail.com*

[2] Department of Mechanical Engineering, Jadavpur University, Kolkata - 700032, West Bengal, India

[3] Department of Instrumentation and Electronics Engineering, Jadavpur University, Kolkata - 700106, West Bengal, India

Received 2020 May 15; accepted 2020 July 23

Abstract The present investigation attempts to quantify the temporal variation of Solar Flare Index (SFI) with other activity indices during solar cycles 21 – 24 by using different techniques such as linear regression, correlation, cross-correlation with phase lag-lead, etc. Different Solar Activity Indices (SAI) considered in this present study are Sunspot Number (SSN), 10.7 cm Solar Radio Flux (F10.7), Coronal Index (CI) and MgII Core-to-Wing Ratio (MgII). The maximum cycle amplitude of SFI and considered SAI has a decreasing trend from solar cycle 22, and cycle 24 is the weakest solar cycle among all other cycles. The SFI with SSN, F10.7, CI and MgII shows hysteresis during all cycles except for solar cycle 22 where both paths for ascending and descending phases are intercepting each other, thereby representing a phase reversal. A positive hysteresis circulation exists between SFI and considered SAI during solar cycles 22 and 23, whereas a negative circulation exists in cycles 21 and 24. SFI has a high positive correlation with coefficient values of 0.92, 0.94, 0.84 and 0.81 for SSN, F10.7, CI and MgII respectively. According to cross-correlation analysis, SFI has a phase lag with considered SAI during an odd-number solar cycle (solar cycles 21 and 23) but no phase lag/lead during an even-numbered solar cycle (solar cycles 22 and 24). However, the entire smoothed monthly average SFI data indicate an in-phase relationship with SSN, F10.7 and MgII, and a one-month phase lag with CI. The presence of those above characteristics strongly confirms the outcomes of different research work with various solar indices and the highest correlation exists between SFI and SSN as well as F10.7 which establishes that SFI may be considered as one of the prime activity indices to interpret the characteristics of the Sun's active region as well as for more accurate short-range or long-range forecasting of solar events.

Key words: Methods: data analysis — Methods: statistical — Sun: activity — Sun: flares — Sun: general

1 INTRODUCTION

All time-dependent short as well as long-lived physical disturbances driven by the magnetic field of the Sun are known as solar activity and some of those are measured in terms of Solar Activity Indices (SAI) at different frequencies. Heliophysicists have made several attempts to quantify the temporal variation of these SAI emanating from different layers of the Sun. This variation in solar activity cycle provides useful information about the physical phenomenon behind those changes in the active region of the Sun. The SAI manifest themselves in an equivocal relationship with others, depending on their origin in the atmosphere of the Sun such as the photosphere, chromosphere and corona. Their relationship with each other varies in different solar activity cycles depending on the cycle characteristics. It has been noted that Solar Cycle 23 is one of the most unusual and longest solar cycles during more than two hundred years of directly measuring SAI (de Toma et al. 2004; Kleeorin et al. 2016). This cycle has lasted for more than 12 years which is higher than half of the Hale magnetic cycle (∼22 years). The maximum value of some SAI like sunspot group activity (Javaraiah 2012), solar flare index (SFI, Roy et al. 2020), etc., during cycle 23 is less than cycle 22 which violates Gnevyshev-Ohl's rule. Also, solar cycle 24 has been a very weak cycle so far (Basu 2013). Nagovitsyn et al. (2012) and Penn & Livingston (2006) pointed out that the average values of both small and large sunspots have decreased gradually during the descending phase of cycle 23 and ascending phase of cycle 24. However, Kilcik et al. (2011) and Lefèvre & Clette (2011) have affirmed that large sunspots remained unaffected during cycle 23 whereas small sunspots have dramatically decreased during the maximum phase of cycle 23. As a result of this, the average sunspot number (SSN) has decreased gradually from cycle 23. Svalgaard et al. (2011) demonstrated that decreasing SSN implies that the temperature of sunspots compared with the outside photosphere is less which makes these spots too small to be observed. It was also pointed out that without a dark sunspot, the Total Solar Irradiance and other SAI might get higher. Janardhan et al. (2010) noted that flaring activity during cycle 23 is weaker than in cycle 21. It has also been pointed out that the magnetic field in the polar region exhibited an unusual fall in its strength during cycle 23 compared to cycles 22 and 21. So, it can be concluded that the highest minimum began during the minimum phase of solar cycle 23 and it continues in solar cycle 24 as well.

It has also been observed that the relationship between two SAI differs during the ascending and descending phases of the 11-year solar cycle due to the presence of hysteresis (Bruevich et al. 2014). The hysteresis represents a common feature of an astronomical process where the magnetic field development is governed by different cyclic activities (Watanabe & Hinteregger 1962; Ching & Chiu 1973; Bachmann & White 1994). Hysteresis of the solar dynamo influences the fluxes of solar extreme ultraviolet radiation which causes a severe effect on the relationship between different solar activities at certain levels as well as on the Earth's atmosphere. This hysteresis has also been observed in the Hα flare index and other SAI such as sunspot area, Coronal Index (CI), etc. during solar cycle 21. However, this phenomenon was absent during solar cycle 22 between Hα flare index and sunspot area (Özgüç & Ataç 2002). The solar soft and hard X-ray shows a time lag of some months with SSNs during solar cycle 21 (Bromund et al. 1995). This time lag exists only during odd-numbered activity cycles between flaring activity in terms of Hα flare index, soft and hard X-ray flare, and the activity related to sunspots such as Sunspot Number and area, whereas this was absent during the even-numbered activity cycles (Temmer et al. 2003).

The present investigation employed different techniques such as linear regression, correlation, cross-correlation with phase lag-lead, etc., on the SFI with other activity indices to analyze their temporal variation. The time variation of SFI is also compared with other activity indices to compute various trends associated with the Sun. This study may establish that SFI represents the characteristics of the Sun's active region.

2 DATA

The daily total disk SFI is considered for this work which was acquired from Kandilli Observatory from March 1976 to December 2018. This period covers solar cycles 21, 22, 23 and almost the complete solar cycle 24. The concept of SFI was first discovered by Kleczek (1952) as **FI = I** $\times$ **T**, which is roughly proportional to the net emitted flare energy. In the above relationship, **I** symbolizes the scale of optical importance, and **T** represents the duration (in minutes) of the daily flaring activity in H-alpha. The scale of optical importance for SFI depends on its brightness and flaring area. The flaring area is categorized as S, 1, 2, 3 or 4 according to the size of the flare whereas brightness is defined as b= bright, n = normal and f = faint in terms of emission intensity. The complete data sets are available on the web page of the Kandilli Observatory. The other SAI considered in this present analysis are as follows:

1. Sunspot Number (SSN): This activity index provides information about the full disk image of the visible Sun. This activity is calculated by the Sunspot Index Data Center (SIDC).
2. 10.7 cm Solar Radio Flux (F10.7): This activity index deals with radio emission at 2800 MHz frequency (10.7 cm wavelength) from the Sun.
3. Coronal Index (CI): This activity index measures the total emitted energy by the solar corona at 530.3 nm wavelength.
4. MgII Core-to-Wing Ratio (MgII): This activity index effectively represents the prominence-to-corona transition region (PCTR) between the cool, dense core and the hot corona (Levens & Labrosse 2019).

Details on the considered SAI with their considered period are listed in Table 1.

3 COMPARISON BETWEEN SOLAR FLARE INDEX AND CONSIDERED SOLAR ACTIVITY INDICES

Figure 1 displays the time variation of monthly averaged SFI, SSN, F10.7, CI and MgII from March 1976 to December 2018 along with their thirteen month running means superimposed (represented by bold red lines). The

Table 1 Details of the Considered Solar Activity Indices

Solar Activity Indices (SAI)	Location on Solar Disk	Considered Period	Data Source
Solar Flare Index (SFI)	Chromosphere to Corona	March 1976 to December 2018 (Solar Cycles 21 – 24)	Kandilli Observatory
Sunspot Number (SSN)	Photosphere	March 1976 to December 2018 (Solar Cycles 21 – 24)	Sunspot Index Data Center
10.7 cm Solar Radio Flux (F10.7)	Lower Corona and Chromosphere	March 1976 to December 2018 (Solar Cycles 21 – 24)	Dominion Radio Astrophysical Observatory in Penticton, British Columbia
Coronal Index (CI)	Corona	March 1976 to December 2008 (Solar Cycles 21 – 23)	Astronomical Institute, Slovak Academy of Sciences, SK-059 60 Tatranska Lomnica Slovak Republic
MgII Core-to-Wing Ratio (MgII)	Chromosphere	October 1986 to December 2018 (Solar Cycles 22 – 24)	Global Ozone Monitoring Experiment (GOME) solar observatory

SFI represents double peaks characteristic at the solar maximum during solar cycles 22 – 24 and a similar kind of characteristic has also been observed in the considered SAI at the same time frame as listed in Table 2. The theoretical concept behind these double peaks which is also known as Gnevyshev peaks, is the variation in the Babcock-Leighton dynamo process (Karak et al. 2018). It is also observed that the maximum cycle amplitude has a decreasing trend from solar cycle 22 and solar cycle 24 has shown the weakest solar cycle among all other solar cycles (Kleeorin et al. 2016). These variations indicate the highest minimum began during the minimum phase of cycle 23. All the above mentioned attributes establish that the SFI may represent the characteristics of the Sun's active region.

4 STUDY OF HYSTERESIS EFFECT IN SOLAR FLARE INDEX WITH CONSIDERED SOLAR ACTIVITY INDICES

The hysteresis is manifested as an equivocal relationship among various SAI during different phases (ascending or descending) of a solar cycle. In this current investigation, the linear regression model between SFI and considered SAI is separately analyzed during the ascending and descending phases of solar cycles 21 to 24. Figure 2 plots the linear regression models between monthly average F10.7, SSN, CI and MgII versus SFI during the ascending and descending phases of solar cycles 21 to 24 separately. Solid blue and red lines signify the slope of the linear regression models for ascending and descending phases of a particular solar cycle respectively and the coefficients (slope M and intercept C) along with their error are listed in Table 3. The equation for the linear regression model is

$$\mathrm{SAI} = M \times \mathrm{SFI} + C \tag{1}$$

where SAI and SFI are the solar activity indices and solar flare index respectively, M is the slope of the linear regression model and C is the intercept.

It is observed from Figure 2 that all the considered SAI with respect to SFI manifest hysteresis: the path for ascending phase does not match the descending phase of a solar cycle. However, this hysteresis phenomenon is not present during solar cycle 22 in all the considered indices as both paths for the ascending and descending phases intercept each other which signifies a phase reversal. This result is consistent with the result obtained by Özgüç & Ataç (2002).

The counterclockwise circulation in a hysteresis loop is considered as positive circulation which represents a lower slope during the ascending phase as compared to the descending phase of a solar cycle (Özgüç & Ataç 2002). This type of circulation represents a normal feature of any hysteresis loop associated with magnetic material. Similarly, clockwise circulation in a hysteresis loop is considered as negative circulation which represents a higher slope during the ascending phase as compared to the descending phase of a solar cycle. The hysteresis circulations in SFI with SSN, F10.7, CI and MgII during solar cycles 21 to 24 are listed in Table 4. A positive hysteresis circulation exists between SFI and considered SAI during solar cycles 22 and 23, whereas a negative circulation exists in cycles 21 and 24.

A cycle is considered as forward or positively inclined if the overall slope of that cycle has a clockwise movement with respect to the preceding cycle, otherwise that cycle is

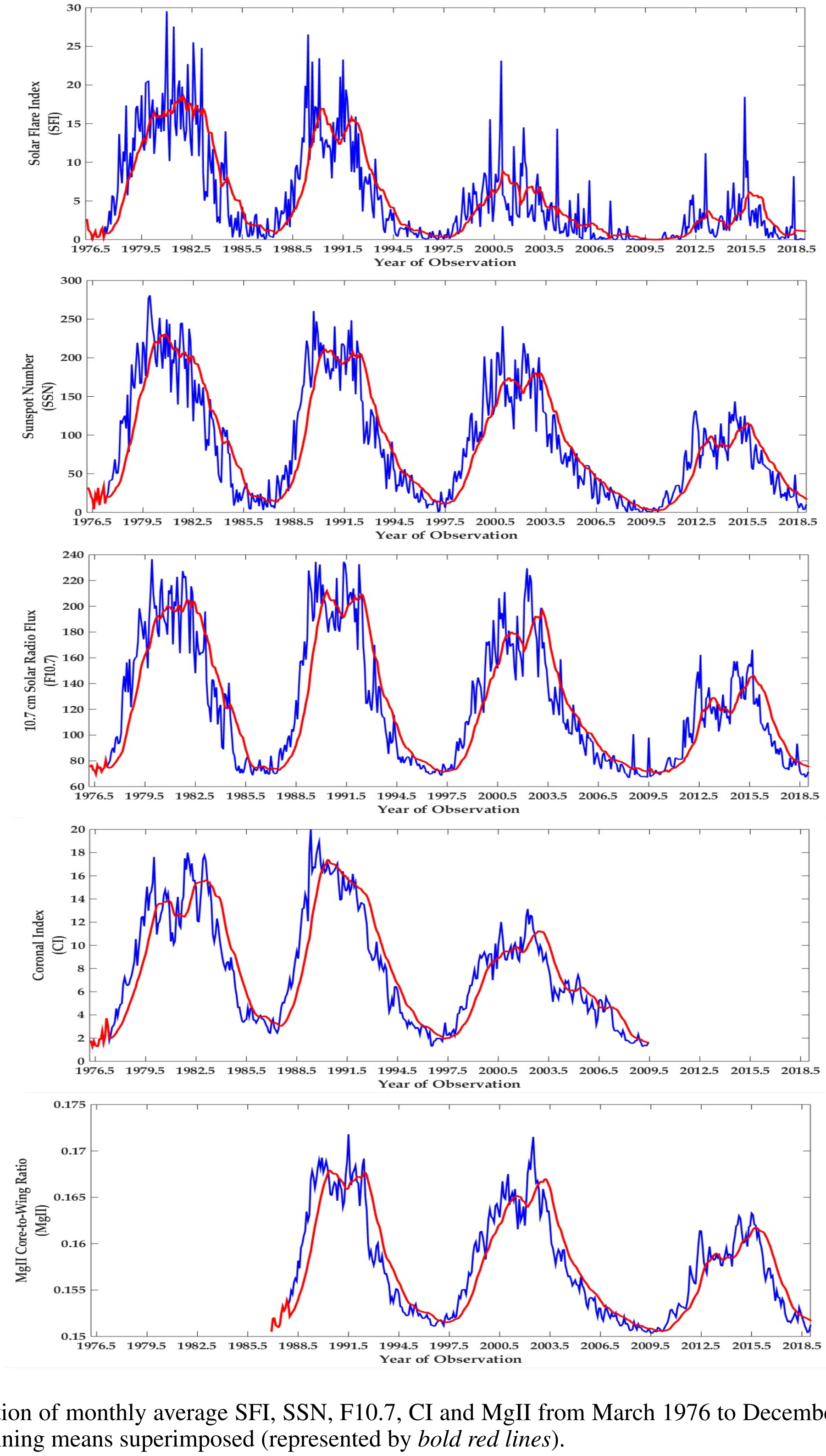

Fig. 1 Time variation of monthly average SFI, SSN, F10.7, CI and MgII from March 1976 to December 2018 with their thirteen month running means superimposed (represented by *bold red lines*).

considered backward or negatively inclined (Özgüç & Ataç 2002). The cycle inclination for SFI with SSN, F10.7, CI and MgII represents the same movement from one cycle to another cycle as shown in Figure 3. A backward or negative inclination exists only from solar cycles 23 to 24, whereas other solar cycles (from 21 to 22 and 22 to 23) have a forward or positively inclined nature.

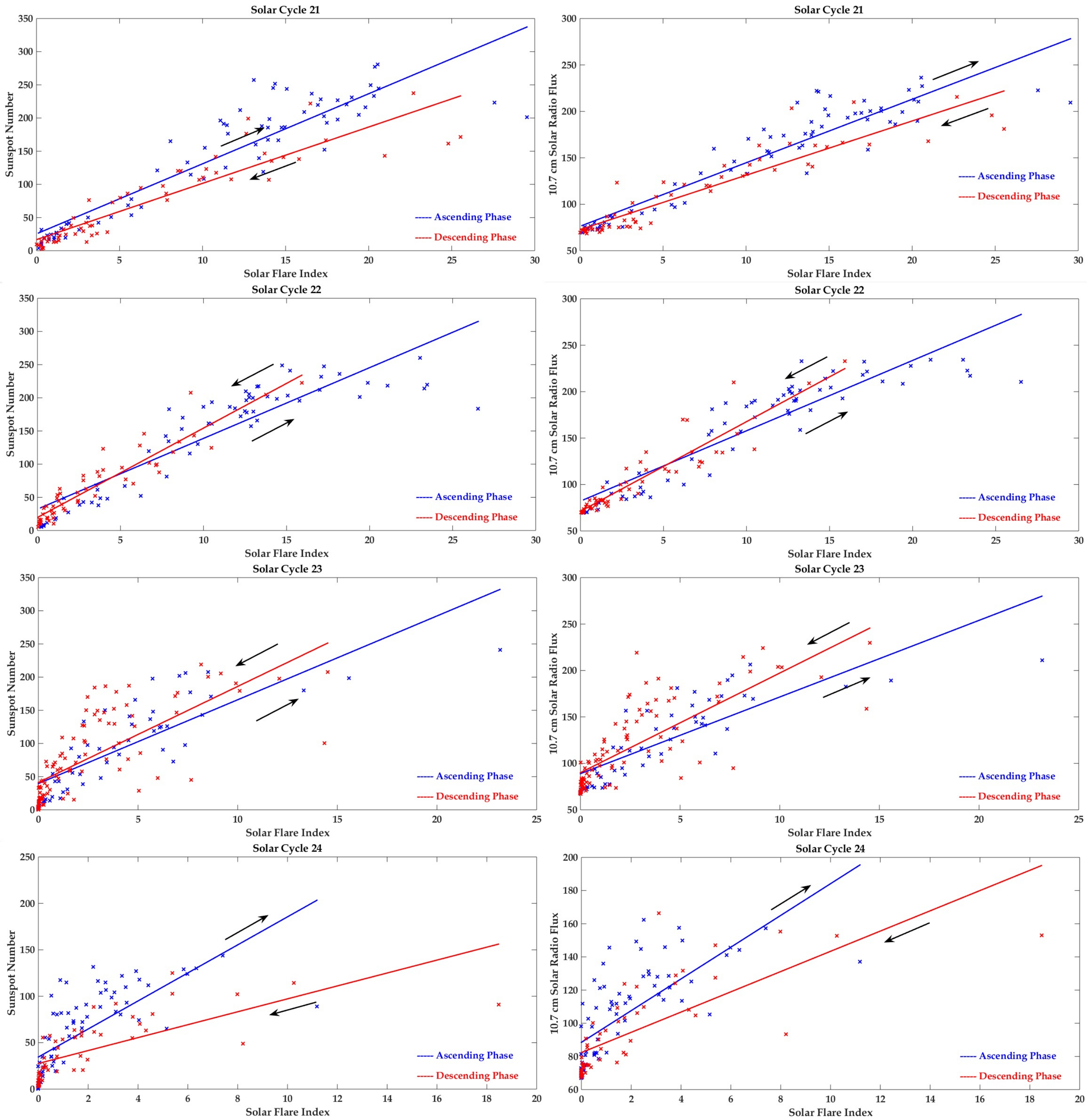

Fig. 2 Linear regression model between monthly averaged F10.7, SSN, CI and MgII versus SFI during the ascending and descending phases of solar cycles 21 to 24.

The overall pattern of those hysteresis loops displays a similar type of trend among all considered indices during solar cycles 21 to 24 but the width of the same varies from cycle to cycle. The hysteresis width is defined as the difference between the ascending and descending paths of a solar cycle. It can be noted that the maximum width exists during solar cycle 24 which may have a significant role.

5 STUDY OF PHASE RELATIONSHIP IN SOLAR FLARE INDEX WITH CONSIDERED SOLAR ACTIVITY INDICES

To interpret the effects related to the hysteresis phenomenon, Bachmann & White (1994) proposed a preliminary concept based on their phase relationship. Later

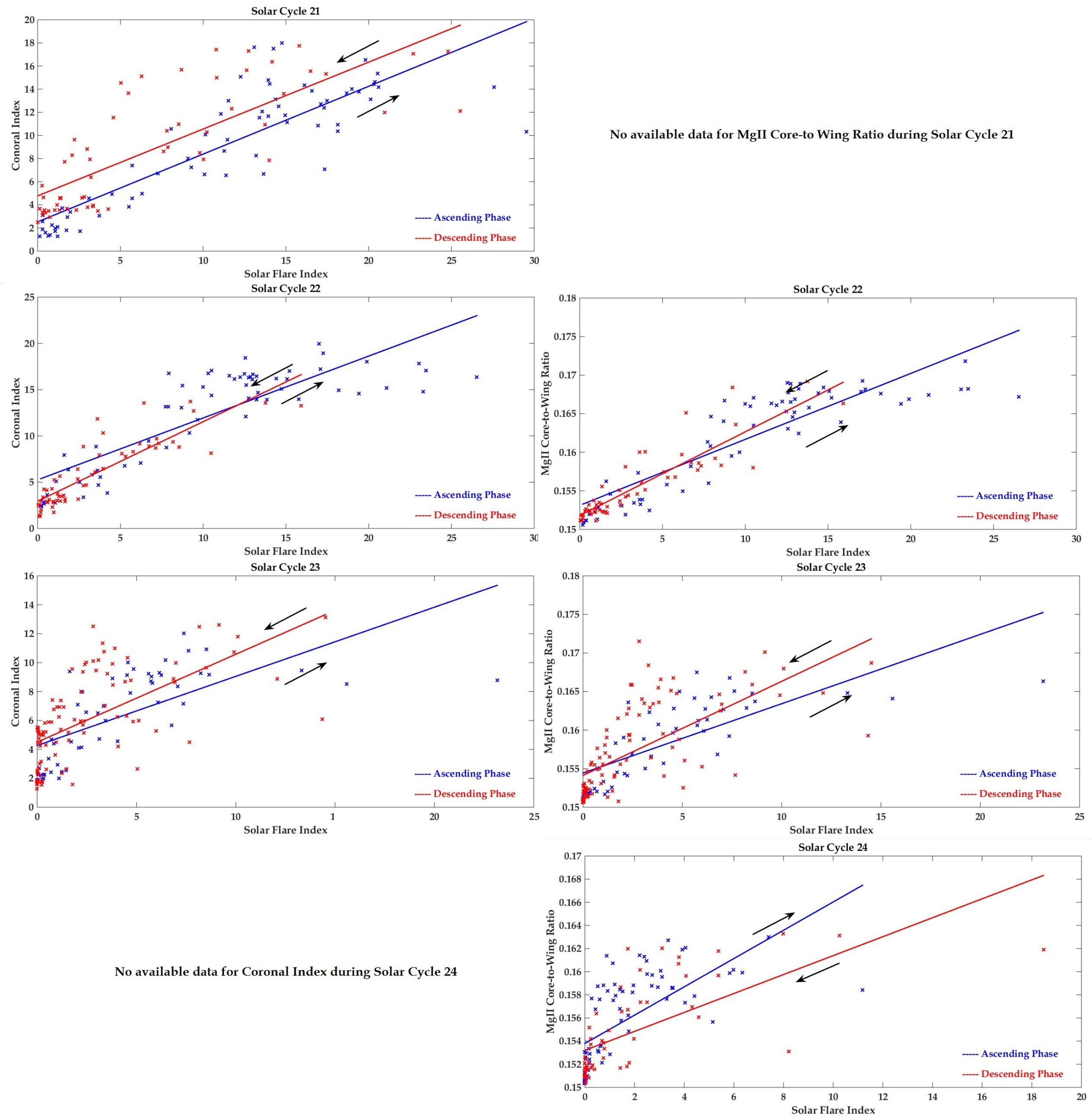

Fig. 2 *Continued.*

Temmer et al. (2003) computed the phase relationship between flare and sunspot related activity and observed some phase lag only during the odd-numbered cycles whereas the even-numbered cycles exhibited an in-phase nature. A similar type of phase relationship is also observed in soft X-ray (Yan et al. 2011) and cosmic ray (Nagashima & Morishita 1980; Van Allen 2000; Cliver & Ling 2001) type of solar indices. The current investigation studies the phase lead-lag relationship between SFI and considered SAI during solar cycles 21 to 24 utilizing a well-known cross-correlation technique. The coefficient $[CC_r(d)]$ is computed for every solar cycle with different lag values (-30 to +30 unit of time). $d < 0$ or $d > 0$ represents a phase lead or lag within the SFI by d points compared to SAI. All the indices are smoothed with a 13 point moving average to rule out the biasing error due to flare production (Yan et al. 2012).

$$CC_r(d) = \frac{\sum_{i=1}^{n}[(\mathrm{SAI}(i) - \overline{\mathrm{SAI}}) \times (\mathrm{SFI}(i-d) - \overline{\mathrm{SFI}})]}{\sqrt{\sum_{i=1}^{n}(\mathrm{SAI}(i) - \overline{\mathrm{SAI}})^2} \times \sqrt{\sum_{i=1}^{n}(\mathrm{SFI}(i-d) - \overline{\mathrm{SFI}})^2}} \tag{2}$$

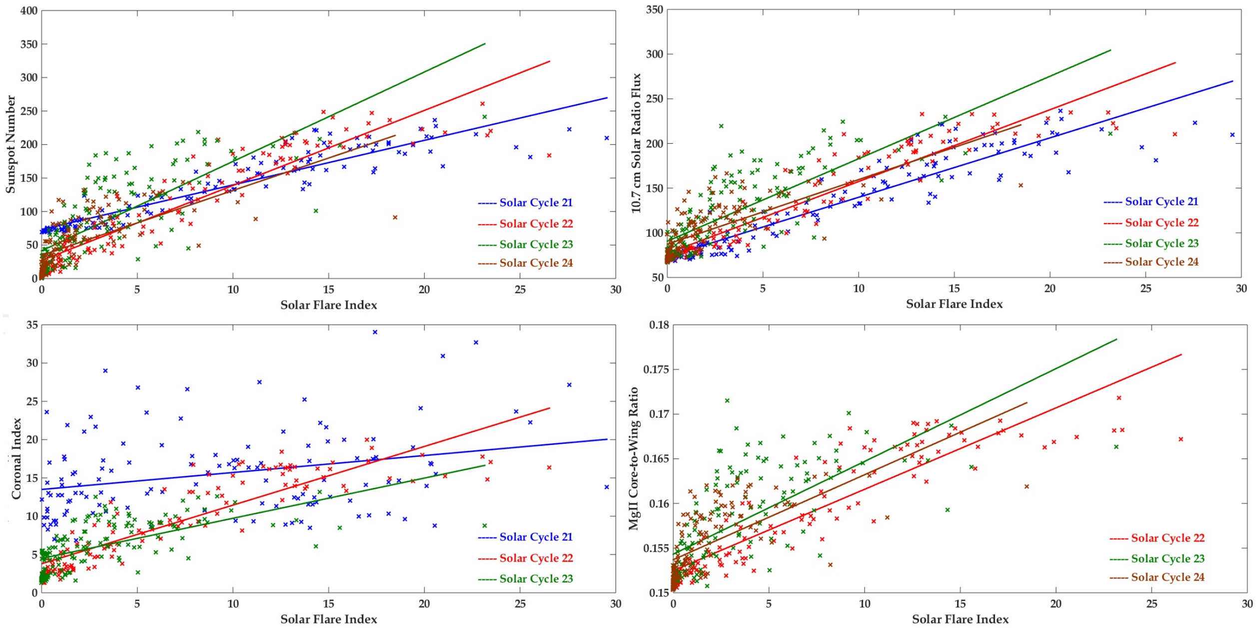

Fig. 3 Linear regression model between monthly average F10.7, SSN, CI and MgII versus SFI during an individual solar cycle.

Table 2 Details of Observed Peaks in the Considered Solar Activity Indices

Solar Indices	Solar Flare Index	Sunspot Number	10.7 cm Solar Radio Flux	Coronal Index	MgII Core-to-Wing Ratio
Solar Cycle 21	Late end of 1981	Late end of 1981	Late end of 1981	Late end of 1980 and Late end of 1982	NA
Solar Cycle 22	Mid of 1990 and Late end of 1991	Mid of 1990 and Late end of 1991	Mid of 1990 and Late end of 1991	Mid of 1990	Mid of 1990 and Late end of 1992
Solar Cycle 23	Mid of 2001 and Late end of 2002	Mid of 2001 and Late end of 2002	Mid of 2001 and Late end of 2002	Mid of 2001 and Late end of 2002	Mid of 2001 and Late end of 2002
Solar Cycle 24	Mid of 2013 and Late mid of 2015	Mid of 2013 and Late mid of 2015	Mid of 2013 and Late mid of 2015	NA	Mid of 2013 and Late mid of 2015

NA: No available data during the considered period.

The cross-correlation plots between SFI and considered SAI during solar cycles 21 to 24 are presented in Figure 4. The phase lag/lead relationship is indicated by the red line which represents the maximum coefficient value of cross-correlation analysis during the considered period and listed in Table 5. A negative (positive) value signifies a backward (forward) phase shift in SFI by d points with respect to the considered SAI. It has been observed that the smoothed monthly average SFI has a phase lag of 3, 3 and 4 months with SSN, F10.7 and CI respectively during cycle 21 and 1, 1, 4 and 1 with SSN, F10.7, CI and MgII respectively during cycle 23. However, no phase lag or lead has been found during solar cycles 22 and 24 except between SFI and CI during cycle 22 which represents a phase lag of one month. So, it can be concluded that SFI has an obvious phase lag during an odd-numbered cycle and no phase lag/lead during an even-numbered cycle. This study also extends this analysis to the entire dataset from cycles 21 to 24 which represents an in-phase relationship with SSN, F10.7 and MgII, and one-month phase lag with CI as plotted in Figure 5.

Temmer et al. (2003) also reported a similar type of phase lag/lead relation with an odd-even solar cycle between flaring activity in terms of soft X-ray as well as Hα and sunspot activity in terms of SSN. Wheatland &

Table 3 Coefficients of Linear Regression Model among Solar Indices and Their Corresponding Errors for Different Phases of Solar Cycles 21 to 24 (SFI versus considered SAI)

Solar Activity with which the linear correlation is computed	Solar Cycle	Phase	*M*	*C*	Error in computing M	Error in computing C
SSN	21	Ascending	10.56	25.43	1.81	3.13
		Descending	8.49	16.70	0.50	4.86
	22	Ascending	10.66	32.22	0.67	8.28
		Descending	13.47	19.60	0.71	3.55
	23	Ascending	12.63	39.55	1.23	7.43
		Descending	14.48	41.19	1.40	5.78
	24	Ascending	15.09	34.55	1.75	4.74
		Descending	6.96	27.61	0.99	3.81
F10.7	21	Ascending	6.84	76.27	0.32	4.19
		Descending	5.85	72.74	0.31	3.04
	22	Ascending	7.57	82.12	0.43	5.26
		Descending	9.65	71.17	0.54	2.68
	23	Ascending	8.25	88.93	0.80	4.85
		Descending	10.72	90.02	0.92	3.78
	24	Ascending	9.57	88.46	1.12	3.03
		Descending	6.10	82.32	0.77	2.94
CI	21	Ascending	0.59	2.53	0.04	0.58
		Descending	0.58	4.78	0.06	0.60
	22	Ascending	0.67	5.25	0.05	0.68
		Descending	0.86	2.95	0.07	0.33
	23	Ascending	0.48	4.27	0.07	0.45
		Descending	0.61	4.50	0.08	0.33
	24	Ascending	NA	NA	NA	NA
		Descending	NA	NA	NA	NA
MgII	21	Ascending	NA	NA	NA	NA
		Descending	NA	NA	NA	NA
	22	Ascending	0.00085	0.153	0.0000598	0.000736
		Descending	0.00108	0.1518	0.0000756	0.000377
	23	Ascending	0.000911	0.1524	0.0000386	0.000373
		Descending	0.00121	0.15413	0.000138	0.00057
	24	Ascending	0.001223	0.1538	0.000168	0.000454
		Descending	0.000818	0.1532	0.0001254	0.000479

NA: No available data during the considered period.

Table 4 The Hysteresis Circulations between SFI and Considered SAI during the Solar Cycles 21 to 24

Solar Activity Indices	Solar Cycle 21	Solar Cycle 22	Solar Cycle 23	Solar Cycle 24
SSN <—> SFI	Negative	Positive	Positive	Negative
F10.7 <—> SFI	Negative	Positive	Positive	Negative
CI <—> SFI	Positive	Positive	Positive	NA
MgII <—> SFI	NA	Positive	Positive	Negative

NA: No available data during the considered period.

Table 5 The Phase Lag/Lead Relation between Smoothed Monthly Averaged SFI and Considered SAI during Solar Cycles 21 – 24

Solar Activity Indices	Solar Cycle 21	Solar Cycle 22	Solar Cycle 23	Solar Cycle 24
SSN <—> SFI	3	0	1	0
F10.7 <—> SFI	3	0	1	0
CI <—> SFI	4	1	4	NA
MgII <—> SFI	NA	0	1	0

NA: No available data during the considered period.

Litvinenko (2001) analyzed the soft X-ray flare with SSNs and found a 6 month lag in the flare. Yan et al. (2011) considered the peak of soft X-ray flare and observed an obvious phase lag during an odd-numbered cycle but no phase lag/lead during an even-numbered cycle with respect to SSN. The current observation is in good agreement with the previous results.

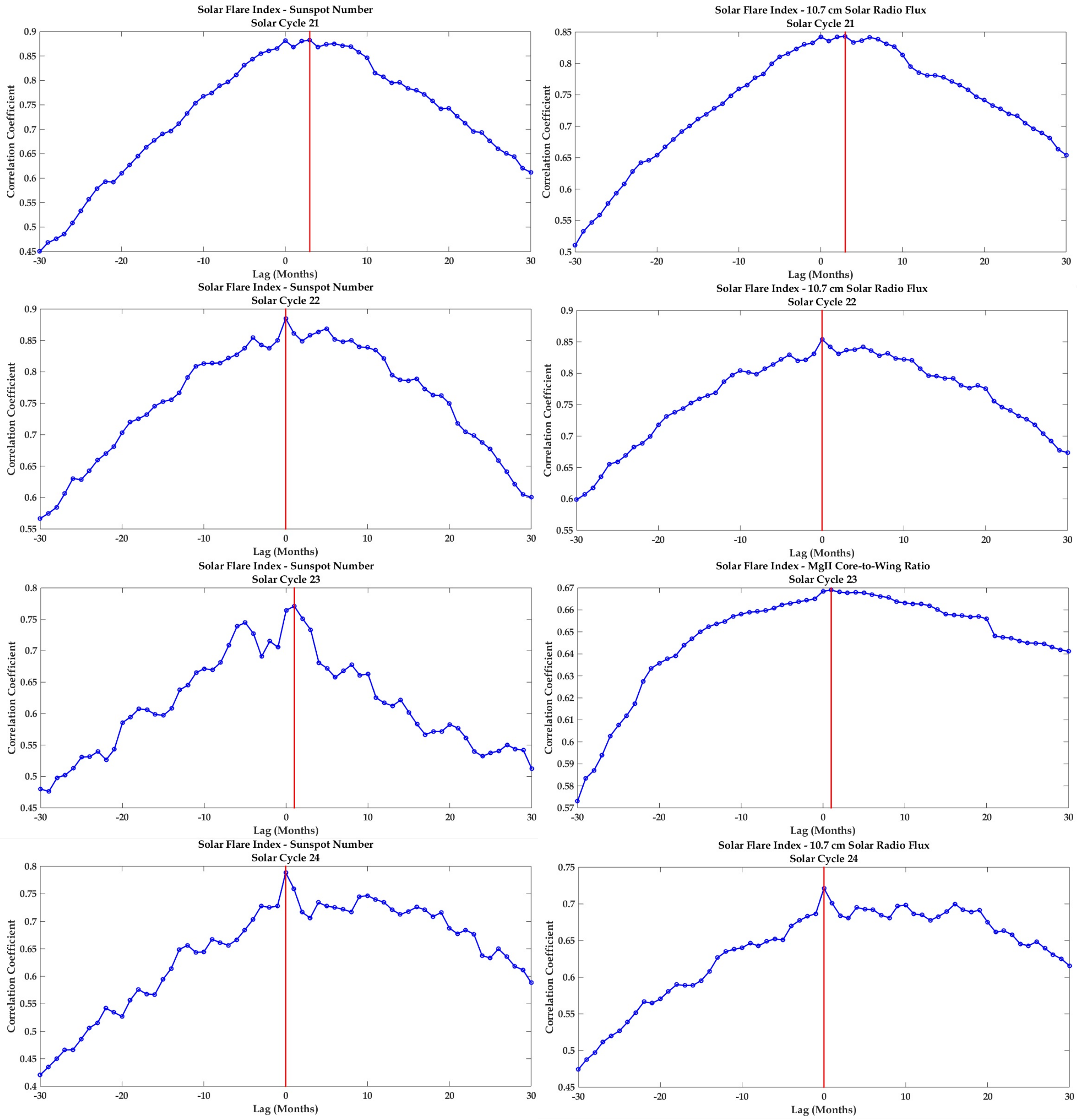

Fig. 4 Cross-Correlation Coefficient between monthly average F10.7, SSN, CI and MgII versus SFI during an individual solar cycle. The red line represents the maximum coefficient value of cross-correlation analysis during the considered period.

6 CORRELATION COEFFICIENT VARIATION BETWEEN SOLAR FLARE INDEX AND CONSIDERED SOLAR ACTIVITY INDICES WITH RESPECT TO TIME

The correlation coefficient is computed between SFI and considered SAI during solar cycles 21 to 24. The probable error of those correlation coefficients is also calculated using the Pearson product-moment method (Eells 2012). The values of those correlation coefficients are 0.92 ± 0.005, 0.94 ± 0.003, 0.84 ± 0.009 and 0.81 ± 0.010 for SSN, F10.7, CI and MgII respectively. These values represent a high positive correlation between SFI and considered SAI. The highest correlation exists between SFI and SSN as well as F10.7 which establishes that SFI can be considered as one of the prime activity indices to study the Sun's active region. The linear regression

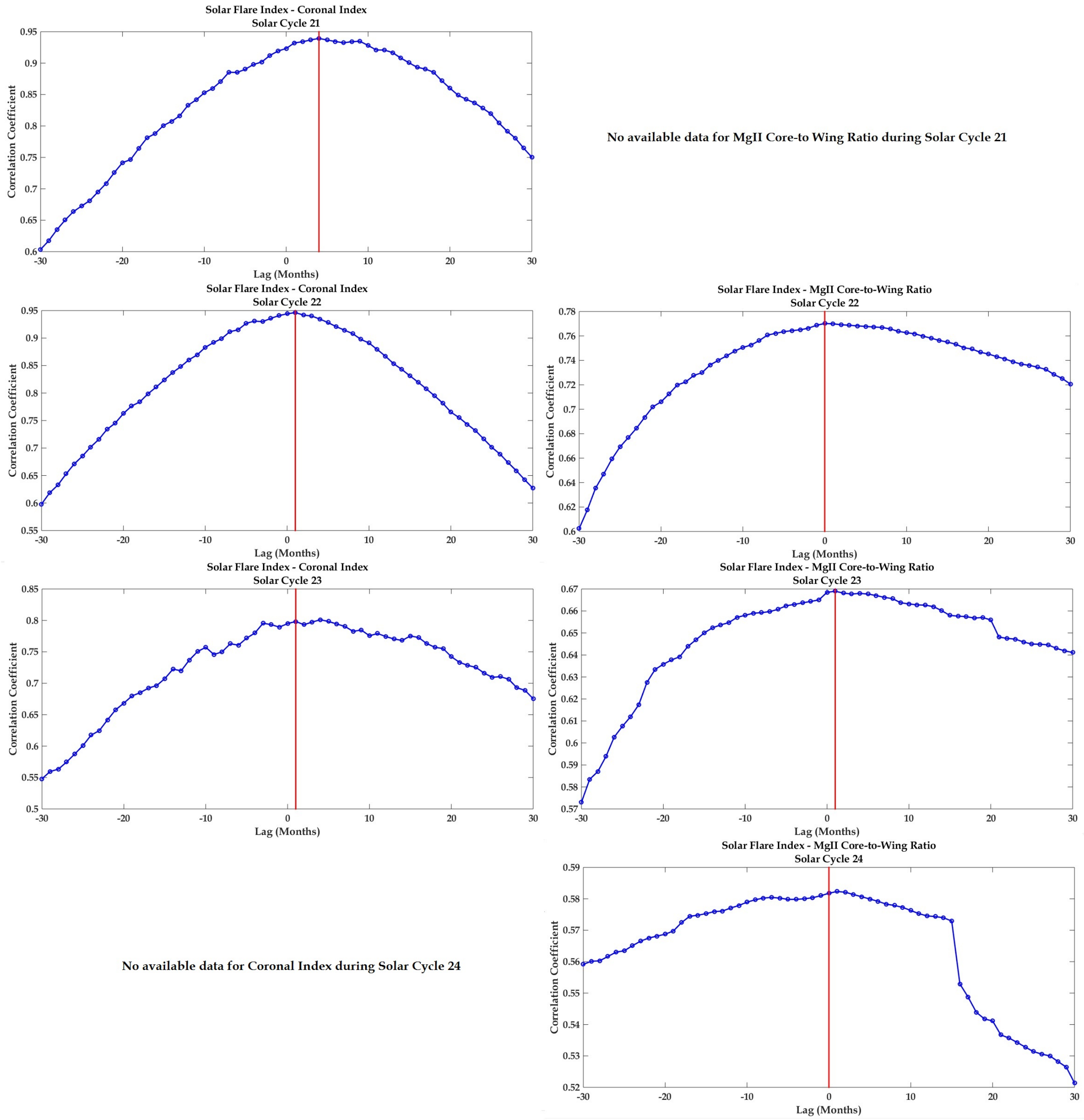

Fig. 4 *Continued.*

equations for those indices are as follows

$$F10.7 = 6.73\text{SFI} + 86.85\,, \tag{3}$$

$$SSN = 10.08\text{SFI} + 35.63\,, \tag{4}$$

$$CI = 0.61\text{SFI} + 4.12\,, \tag{5}$$

$$MgII = 0.00087\text{SFI} + 0.153\,. \tag{6}$$

The correlation coefficient is also computed between SFI and considered SAI for different phases as well as for the complete cycle separately during solar cycles 21 to 24 and listed in Table 6. Those coefficients are within the range from 0.75 to 0.95, which are very close to one. The maximum values, in this case, have been observed for SSN as well as for F10.7 which agrees with the analysis considering the whole dataset.

To identify the variation in correlation with the progress of a solar cycle, the correlation coefficients are

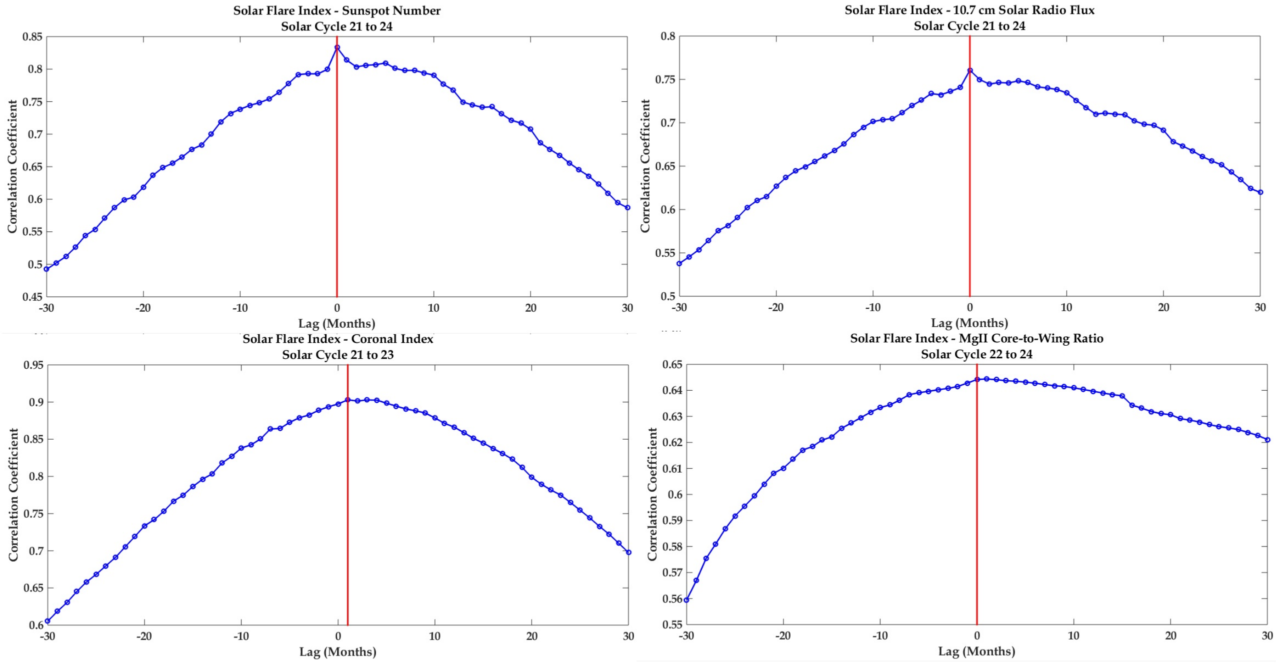

Fig. 5 Cross-Correlation Coefficient between monthly average F10.7, SSN, CI and MgII versus SFI during the whole dataset from solar cycles 21 to 24. The red line represents the maximum coefficient value of cross-correlation analysis during the considered range.

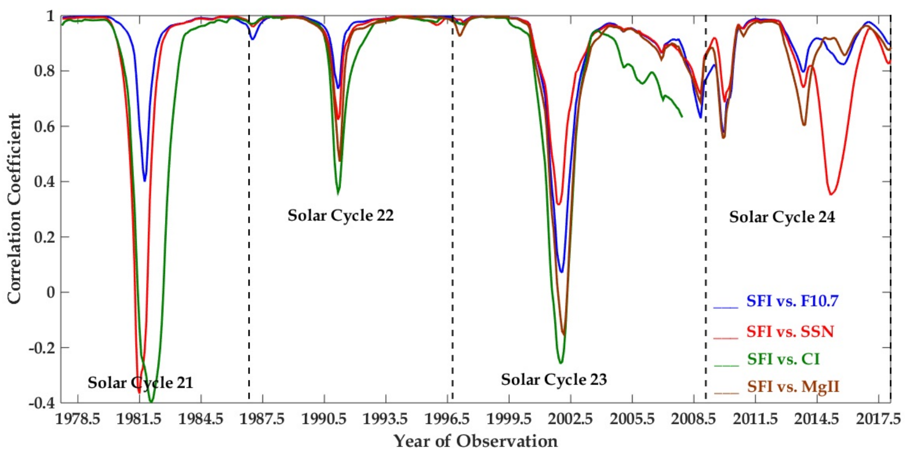

Fig. 6 Correlation coefficient variation between SFI and considered SAI calculated during a three year interval.

calculated for each and every instant of time t (in years) for the time interval (Δt) of 3 years ((t - 1.5 yr) $< \Delta t <$ (t + 1.5 yr)) and are presented in Figure 6. The correlation coefficients between SFI and considered SAI attain their minimum values during cycle maximum or nearly after that (i.e. for cycle 21: 1981.5 to 1985, cycle 22: 1991, cycle 23: 2002 and cycle 24: 2014 to 2015). This is due to the local disturbance of the Sun during the cycle maximum of each solar cycle (Gupta et al. 2007). It can be observed that the variations in correlation coefficient for all the indices attain their minimum and maximum values at the same time during a particular cycle. The logical reason is that all the indices represent the same dynamo process in the Sun. This variation in the correlation coefficient not only captures the physical relation among different SAI but is also helpful in reconstructing SAI depending on their mutual relationship.

7 CONCLUSIONS

The current investigation presents a study of the hysteresis phenomenon, phase relationship and correlation coefficient variation between SFI and other SAI such as SSN, F10.7, CI and MgII from March 1976 to December 2018.

Table 6 The Phase Lag/Lead Relation between Smoothed Monthly Averaged SFI and Considered SAI during Solar Cycles 21 – 24

Solar Activity Indices	Phase	Solar Cycle 21	Solar Cycle 22	Solar Cycle 23	Solar Cycle 24
	Ascending	0.91± 0.014	0.90± 0.016	0.92± 0.014	0.81± 0.027
SSN <—> SFI	Descending	0.91± 0.015	0.93± 0.012	0.83± 0.022	0.80± 0.033
	Total Cycle	0.91± 0.010	0.93± 0.008	0.86± 0.014	0.73± 0.028
	Ascending	0.93± 0.011	0.92± 0.013	0.92± 0.014	0.81± 0.027
F10.7 <—> SFI	Descending	0.93± 0.012	0.93± 0.012	0.87± 0.017	0.84± 0.027
	Total Cycle	0.94± 0.007	0.94± 0.007	0.88± 0.013	0.78 0.024
	Ascending	0.85± 0.022	0.84± 0.025	0.87± 0.023	NA
CI <—> SFI	Descending	0.78± 0.035	0.87± 0.022	0.82± 0.023	NA
	Total Cycle	0.80± 0.021	0.89± 0.013	0.83± 0.017	NA
	Ascending	NA	0.88± 0.019	0.85± 0.026	0.75± 0.035
MgII <—> SFI	Descending	NA	0.89± 0.019	0.78± 0.027	0.77± 0.038
	Total Cycle	NA	0.91± 0.011	0.79± 0.021	0.73± 0.028

NA: No available data during the considered period.

This period covers solar cycles 21, 22, 23 and almost the complete solar cycle 24. Some of the important points of this investigation are as follows:

1. The SFI along with considered SAI displays a double peak nature during the solar maximum of each solar cycle due to the variation in the Babcock-Leighton dynamo process.
2. The maximum cycle amplitude of SFI along with SSN, F10.7, CI and MgII has a decreasing trend from solar cycle 22. These variations indicate the highest minimum began during the end phase of solar cycle 23. Solar cycle 24 has been found to be the weakest solar cycle among all the solar cycles.
3. SFI with SSN, F10.7, CI and MgII show hysteresis during every cycle except for solar cycle 22 where both paths for ascending and descending phases are intercepting each other thereby representing a phase reversal. A positive hysteresis circulation exists between SFI and considered SAI during solar cycles 22 and 23, whereas a negative circulation exists in cycles 21 and 24.
4. A backward or negative cycle inclination is present only from solar cycles 23 to 24 between SFI and considered SAI, whereas other solar cycles (from 21 to 22 and 22 to 23) display a forward or positive cycle inclined nature.
5. The SFI has an obvious phase lag with SSN, F10.7 and MgII during an odd-numbered solar cycle but no phase lag/lead during an even-numbered solar cycle. However, the entire smoothed monthly average SFI data indicate an in-phase relationship with SSN, F10.7 and MgII, whereas a one-month phase lag with CI.
6. The correlation coefficients between SFI and other SAI during solar cycles 21 to 24 are 0.92±0.005, 0.94±0.003, 0.84±0.009 and 0.81±0.010 for SSN, F10.7, CI and MgII respectively. This value indicates a good positive correlation of SFI with respect to considered SAI. Also, the variations of correlation coefficient attain their minimum values during cycle maximum or nearly after that due to the local disturbance of the Sun during cycle maximum of each solar cycle.

The presence of those above characteristics strongly confirms the outcomes of different research work with various solar indices and establishes that the SFI have similar attributes during solar cycles 21 to 24 along with other solar indices which represent the characteristics of the Sun's active region. Also, the highest correlation exists between SFI and SSN as well as F10.7 which establishes that the SFI may be considered as one of the prime activity indices to interpret the nature of the Sun's active region as well as for more accurate short-range or long-range forecasting of solar events. The present cycle has already shown an awfully quiet and extended solar minimum and the polar magnetic fields were weak during the solar cycle 24 minimum compared to those during the solar cycle 23 minimum (Basu 2013). Also, the Sun has manifested unusual behavior during solar cycle 23. To understand those peculiarities in solar internal dynamics, future study should incorporate the study of solar oscillation frequencies which significantly change with solar activity (Christensen-Dalsgaard 2002; Basu 2013) along with the study of SFI to reveal better insights into the solar internal dynamics.

Acknowledgements We are thankful to the National Geophysical Data Center (NGDC) as well as Kandilli Observatory, Sunspot Index Data Center, Dominion Radio Astrophysical Observatory in Penticton, British Columbia, Astronomical Institute, Slovak Academy of Sciences, SK-059 60 Tatranska Lomnica Slovak Republic, and the Global Ozone Monitoring Experiment (GOME) solar observatory for providing us the data for this analysis. We sincerely acknowledge the support extended by Jadavpur University, West Bengal India. This work is a part of the RUSA 2.0 faculty major research project under Jadavpur University.

References

Bachmann, K. T., & White, O. R. 1994, Sol. Phys., 150, 347
Basu, S. 2013, in Journal of Physics Conference Series, 440, Journal of Physics Conference Series, 012001
Bromund, K. R., McTiernan, J. M., & Kane, S. R. 1995, ApJ, 455, 733
Bruevich, E. A., Bruevich, V. V., & Yakunina, G. V. 2014, Journal of Astrophysics and Astronomy, 35, 1
Ching, B. K., & Chiu, Y. T. 1973, Journal of Atmospheric and Terrestrial Physics, 35, 1615
Christensen-Dalsgaard, J. 2002, Reviews of Modern Physics, 74, 1073
Cliver, E. W., & Ling, A. G. 2001, ApJL, 551, L189
de Toma, G., White, O. R., Chapman, G. A., et al. 2004, ApJ, 609, 1140
Eells, W. C. 2012, Journal of the American Statistical Association, 241929, 170
Gupta, M., Mishra, V. K., & Mishra, A. P. 2007, Journal of Geophysical Research (Space Physics), 112, A05105
Janardhan, P., Bisoi, S. K., & Gosain, S. 2010, Sol. Phys., 267, 267
Javaraiah, J. 2012, Sol. Phys., 281, 827
Karak, B. B., Mandal, S., & Banerjee, D. 2018, ApJ, 866, 17
Kilcik, A., Yurchyshyn, V. B., Abramenko, V., et al. 2011, ApJ, 731, 30
Kleczek, J. 1952, Bull. Astron. Inst. Czech, 3, 52
Kleeorin, Y., Safiullin, N., Kleeorin, N., et al. 2016, MNRAS, 460, 3960
Lefèvre, L., & Clette, F. 2011, A&A, 536, L11
Levens, P. J., & Labrosse, N. 2019, A&A, 625, A30
Nagashima, K., & Morishita, L. 1980, Planet. Space Sci., 28, 195
Nagovitsyn, Y. A., Pevtsov, A. A., & Livingston, W. C. 2012, ApJL, 758, L20
Özgüç, A., & Ataç, T. 2002, in Solar-Terrestrial Magnetic Activity and Space Environment, eds. H. Wang & R. Xu, 14, 447
Penn, M. J., & Livingston, W. 2006, ApJL, 649, L45
Roy, S., Prasad, A., Ghosh, K., Panja, S. C., & Patra, S. N. 2020, Sol. Phys., 295, 100
Svalgaard, L., Lockwood, M., & Beer, J. 2011, ISSI team, 233, *http://www.leif.org/research/svalgaard_ISSI_Proposal_Base.pdf*
Temmer, M., Veronig, A., & Hanslmeier, A. 2003, Sol. Phys., 215, 111
Van Allen, J. A. 2000, Geophys. Res. Lett., 27, 2453
Watanabe, K., & Hinteregger, H. E. 1962, J. Geophys. Res., 67, 999
Wheatland, M. S., & Litvinenko, Y. E. 2001, ApJ, 557, 332
Yan, X. L., Deng, L. H., Qu, Z. Q., & Xu, C. L. 2011, Ap&SS, 333, 11
Yan, X. L., Deng, L. H., Qu, Z. Q., Xu, C. L., & Kong, D. F. 2012, Journal of Astrophysics and Astronomy, 33, 387